Journal of the Korean Ceramic Society
Vol. 54, No. 1, pp. 28~32, 2017.

https://doi.org/10.4191/kcers.2017.54.1.01

Novel Synthesis and Characterization of Pt-graphene/TiO_2 Composite Designed for High Photonic Effect and Photocatalytic Activity under Visible Light

Shu Ye and Won-Chun Oh†

Department of Advanced Materials Science and Engineering, Hanseo University, Seosan 31962, Korea

(Received June 19, 2016; Revised November 29, 2016; Accepted December 1, 2016)

ABSTRACT

The degradation of methyl blue (MB) catalyzed by platinum (Pt)-graphene/TiO_2 in dark ambiance was studied. Pt–graphene/TiO_2 composites were prepared by simple hydrothermal method. Characterizations of composites were studied by X-ray diffraction (XRD), scanning electron microscopy (SEM), transmission electron microscopy (TEM), specific surface area (BET) analysis, and energy dispersive X-ray (EDX) analysis. UV-spectroscopic analysis of the dyes was performed by measuring the change in absorbance. The degradation of the organic dyes was calculated based on the decrease in concentration of the dyes with respect to regular time intervals. Rate coefficients for the catalytic process were successfully established and reusability tests were performed to test the stability of the used catalysts.

Key words : Graphene, TiO_2, TEM, Raman, Dyes

1. Introduction

Titanium dioxide is the most investigated functional material in the family of semiconductor photocatalysts.[1-5] It has been observed previously that the nanocomposites of titanium dioxide and carbon, including activated carbon, carbon nanotubes (CNTs), and fullerenes, are able to induce enhanced photocatalytic performance beyond that of TiO_2 only. The combination of graphene oxide with other photocatalyst materials has been considered in studying the photocatalytic effect and enhanced catalytic activities have been found.[6-8] In particular, graphene-based materials have attracted considerable attention because of their high thermal conductivity (~ 5000 W m^{-1} K^{-1}), excellent charge mobility at room temperature (200000 cm^2 $V^{-1}s^{-1}$), and extremely high theoretical specific surface area (~2600 m^2g^{-1}).[9-14] These properties make graphene an excellent material in photocatalysts to increase the charge transfer separation of generated electron and holes.[15-16]

For enhancement of catalytic activity, the dispersion of catalyst particles on graphene sheets can provide new ways to increase the catalyst performance in energy conversion devices. Enhanced electrocatalytic activity of Pt nanoparticles dispersed on the carbon nanotubes has already been reported.[17-18] Herein we report a facile and fast way to synthesize Pt–graphene/TiO_2 via an ultrasonic assisted method in which graphene oxide is mixed with Pt and the resulting solution is ultra-sonicated for 30 min; this is followed by mixing with the TiO_2 precursor material. In this process, in ethylene glycol solution, simultaneous reduction of graphene oxide into graphene and attachment of noble metal nanoparticles to TiO_2 are observed. For comparison of photocatalytic effect, the photocatalytic activity of the Pt–graphene/TiO_2 hybrid material was tested using methyl blue (MB) as a model contaminant under visible light. The results indicate a promising development toward a graphene based, efficient photocatalyst that employs visible light as an energy source.

†Corresponding author : Won-Chun Oh
E-mail : wc_oh@hanseo.ac.kr
Tel : +82-41-660-1337 Fax : +82-41-688-3352

2. Experimental Procedure

2.1. Materials

Titanium (IV) n-butoxide (TNB, $C_{16}H_{36}O_4Ti$) used as a titanium source was purchased from Kanto Chemical Company (Tokyo, Japan). Hydrogen hexachloroplatinate (IV) hydrate ($H_2PtCl_6{\cdot}nH_2O$ n = 5.5) was used as a platinum source and was purchased from Kojima Chemical Co., Ltd., Japan. Methyl blue (MB) was used as model pollutant and was purchased from Samchun Pure Chemical Co., Ltd., Korea. Ethylene glycol was purchased from Dae-Jung Chemical and Metals Co., Ltd., Korea. All chemicals were used without further purification.

2.2. Synthesis of graphene oxide

In brief, 10 g of natural graphite powder were mixed with conc. H_2SO_4 (230 ml) at 0°C with vigorous magnetic stirring. In the next step, 30 g of $KMnO_4$ was slowly added to the flask and the temperature was kept below 15°C. The resulting mixture was stirred at 35°C until it became pasty and brownish; it was then diluted to 150 ml using de-ionized

(DI) water and stirring was maintained at a temperature below 90°C. After adding water, the container was sealed and kept at 100°C with vigorous stirring for 30 min; this was followed by the addition of 20% H_2O_2 drop by drop within 5 min. The mixture was then washed several times with water, acetone and 10% HCl solution to eliminate residual metal ions. The mixture was heat treated in dry oven at 90°C for 12 h to obtained graphite oxide powder. For the preparation of graphene oxide, 200 mg of graphite oxide powder were mixed in 200 ml DI water (1 mg/ml) with stirring for 30 min and mixture was ultrasonicated (using 750 W, Ultrasonic Processor VCX 750, Korea) for 2 h. The resulting solutions were filtered and washed several times with hot water and kept in a dry oven for 6 h to achieve graphene oxide powder.

2.3. Synthesis of Pt/TiO_2

0.05 mmol H_2PtCl_6 and 100 mg graphene powder were dispersed in EG solution (20.0 mL) under vigorous stirring to form a stable suspension. This step was followed by constant stirring and ultrasonication for 40 min. After completion, the black solution was filtered, washed 3 times with deionized water and ethanol, and then dried at 100 °C. Finally, the sample was heated at 600°C for 1 h. The obtained sample was named Pt/TiO_2.

2.4. Synthesis of Pt-graphene/TiO_2

0.05 mmol H_2PtCl_6, 100 mg graphene oxide powder, and 2 ml TNB were dispersed in EG solution (20.0 mL) under vigorous stirring to form a stable suspension; this was followed by constant stirring and ultrasonication for 40 min. After completion, the black solution was filtered, washed 3 times with deionized water and ethanol, and then dried at 100 °C. Finally, the sample was heated at 600°C for 1 h. The obtained sample was named Pt-graphene/TiO_2.

2.5. Dye adsorption experiments using visible light

The photocatalytic activity of the as-prepared Pt-graphene supported TiO_2 nanocomposites was evaluated by the degradation of MB under visible light. A LED lamp (8W, $\lambda > 420$ nm, KLD-08L LED lamp) served as the simulated visible light source. In each run, 10 mg of the Pt-graphene/TiO_2 catalytic sample was added to a 50 ml solution of MB (0.1 mg ml^{-1}). To obtain adsorption–desorption equilibrium, the solution was kept in the dark for 2 h. Before the LED lamp was switched on, a sample was collected from the solution and kept in a centrifuge at 1000 rpm for the removal of solid material. Afterwards, the LED lamp was switched on and samples were collected periodically. At certain time intervals, the collected samples were immediately centrifuged for 10 minutes to remove the solid material for further analysis. Each photocatalyst composite was irradiated for 150 minutes to determine its catalytic efficiency.

2.6. Characterization

The fabrication of the samples was carried out in an ultrasonic chamber with an ultrasonic generator. The ultrasonic generator had the following specifications: model no: VCX, 750 - 750 Watts, frequency: 20 kHz, remote actuation compatible, dimensions (H × W × D) 91/4" × 71/2" × 131/2" (235 × 190 × 340 mm), weight: 15 lbs. (6.8 kg), with a standard probe having a temperature up to 100°C, tip diameter: 1/2" (13 mm), with threaded end and replaceable tip. The crystal structures and phases of the samples were obtained by XRD (Shimata XD-D1, Japan) with Cu Ka radiation in the range of 2 theta from 10 to 80, at a scan speed of 1.20 m1. Energy dispersive X-ray spectroscopy (EDX) was also employed for elemental analysis. The morphology of the sample was studied by SEM (JSM-5200 JOEL, Japan). Transmission electron microscopy (TEM, JEOL, JEM-2010, Japan) was used to observe the surface state and structure of the photocatalyst composites. TEM was also used to examine the size and distribution of the Pt particles deposited on the graphene sheet. Raman analysis was carried out to check for the signature of graphene in the samples. The measurement was performed using a labRam Aramis Horiba Jobin Yvon spectrometer. A 514 nm argon-ion laser was used for the measurements. The measurements were performed using backscattering geometry. The Raman excitation beam spot size had a diameter of about 1 μm.

3. Results and Discussion

3.1. Characterization of TiO_2, Pt/TiO_2, and Pt-graphene/TiO_2 samples

Figure 1 shows the XRD patterns of the TiO_2, Pt/TiO_2, and Pt-graphene/TiO_2 samples. In this figure, the (002) diffraction peak of graphene shifts to a higher angle. The XRD patterns of the Pt-graphene/TiO_2 nanocomposites show strong diffraction peaks at 39.7, 46.0, 67.4, 80.1, and 85.0, which are in good agreement with the (111), (200), (220), (311), and (222) crystal planes of pure Pt with face-centered-cubic (fcc) phase (JCPDS 65-2868).[19-21] From the XRD spectra, the position of the (002) diffraction peak at 26.2 indicates that graphene is further converted to crystalline graphene, and

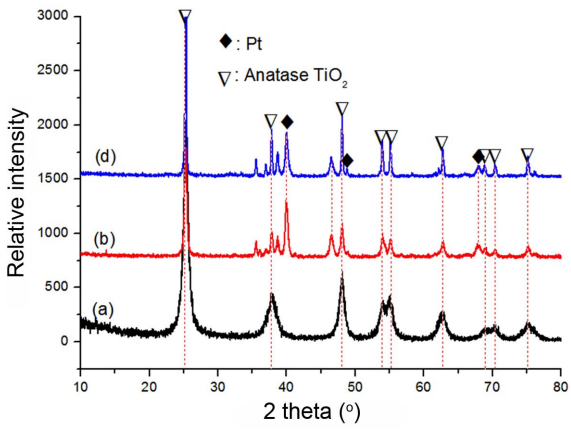

Fig. 1. XRD pattern of as-prepared samples: (a) TiO_2, (b) Pt/TiO_2, (c) Pt-graphene/TiO_2.

Table 1. Energy Dispersive X-ray Elemental Microanalysis (wt%) of TiO_2, Pt/TiO_2, and Pt-graphene/TiO_2 Samples

Sample \ Element	C	O	Pt	Ti	Impurity	Total
TiO_2	0.00	45.22	0.00	54.36	0.42	100.00
Pt/TiO_2	0.00	48.16	7.69	43.81	0.34	100.00
Pt-graphene/TiO_2	49.47	24.19	4.73	21.03	0.58	100.00

that the conjugated graphene network (sp2 carbon) has been reestablished.[22-23] This also confirms that the ultrasonic process did not destroy the graphene structure.

Table 1 lists the numerical results of the EDX quantitative microanalysis of the samples. In the whole set of spectra, the C elemental peak originates from the graphene sheet. The titanium and oxygen in the figure arise from the TiO_2 precursor material. Elemental Pt came from H_2PtCl_6.

The morphology of Pt/TiO_2 is shown in Fig. 2(a,b). A homogeneous distribution with some agglomeration was observed. SEM images of Pt-graphene/TiO_2 are shown in Fig. 2(c,d); they exhibited the well-known properties of surface nanostructures. This suggests that Pt and TiO_2 particles were well-dispersed on the layered graphene nanosheet. Due to van der Waals interaction, the graphene sheet tends to aggregate back to the graphite structure; functionalizing with nanoparticles is helpful to overcome these interactions.[24-25] For the TiO_2 particles, the graphene sheet acts like a bridge, which may be beneficial to provide a path for the photo generated electrons and hence to enhance the catalytic performance.[26]

TEM images were taken of each sample to enhance the structural investigation in nanoscale, as shown in Fig. 3. In the TEM images for the Pt/TiO_2 sample (Fig. 3(b)), TiO_2 particles do not appear as clear shapes surrounded by Pt particles. As shown in Fig. 3(b), the Pt particles were closely attached to the TiO_2 surface, which makes it appear darker. The Pt particles were the smaller particles unevenly distributed on the graphene sheets as well. As shown in Fig. 3(c), the Pt particles can be observed to be highly agglomerated, forming clusters of composites and making that area possess a darker image that is almost blackened, while the TiO_2 particles were larger spherical structures compared to the Pt particles, which produce a lighter image.[27-28] This indicates that the process of TEM imaging of the Pt-graphene/TiO_2 composites was acceptable. All the dispersion states of this group of samples were very high.

Figure 4 shows the Raman spectra of the Pt-graphene/TiO_2 sample. The variation in the Raman band intensity and the shift provide information on the nature of C–C bonds and defects. The Raman spectra show the characteristic D and G bands at 1354 and 1590 cm^{-1} found in graphene. The D band is a common feature for sp^3 defects in carbon, and the G band provides information on in-plane vibrations of sp^2 bonded carbons.[29-34] The Pt-graphene/TiO_2 nanocomposite showed a D band and a G band; this proves the existence of graphene.

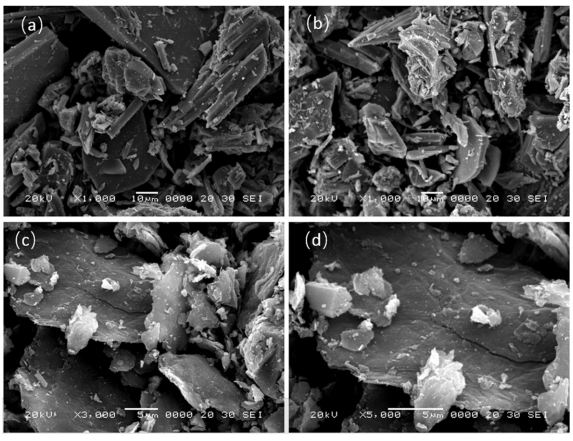

Fig. 2. SEM micrographs of as-prepared samples. (a,b) Pt/TiO_2; (c,d) Pt-graphene/TiO_2.

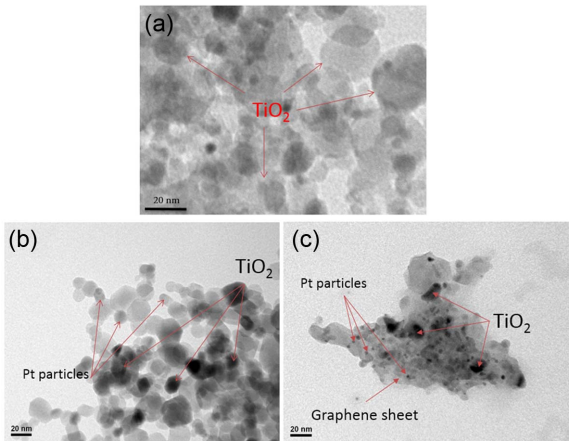

Fig. 3. TEM images of (a) TiO_2, (b) Pt/TiO_2, and (c) Pt-graphene/TiO_2 sample.

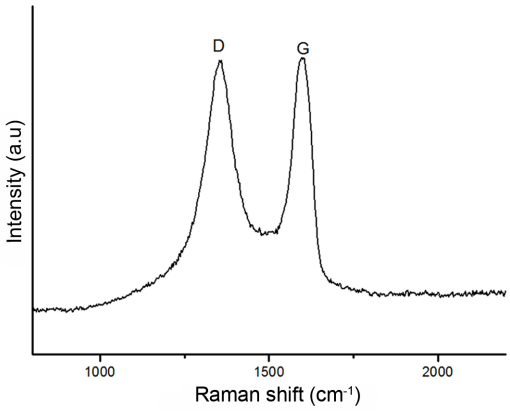

Fig. 4. Raman spectra of Pt-graphene/TiO_2 composite.

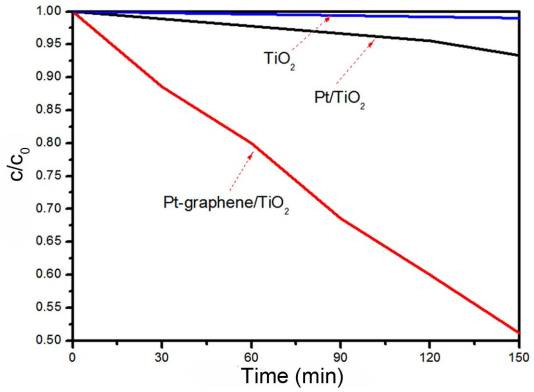

Fig. 5. Degradation of MB under visible light irradiation with magnetic stirring over TiO_2, Pt/TiO_2, and Pt-graphene/TiO_2. c is the concentration of MB solution, and c_0 is the initial concentration.

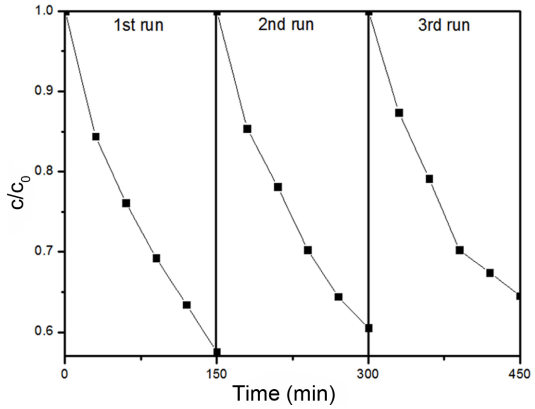

Fig. 6. Cycling runs for the photocatalytic degradation of MB with Pt-graphene/TiO_2 sample under visible light irradiation.

3.2. Novel Photonic Performance of MB

Figure 5 shows the MB degradation versus time using TiO_2, Pt/TiO_2, and Pt-graphene/TiO_2 under visible light. The spectra for the MB solution after visible light irradiation showed relative degradation yields at different irradiation times. The dye concentration continuously decreased with a gentle slope; this was due to visible light irradiation. The concentration of MB was 5.0×10^{-5} mol/L; the absorbance of MB decreased with increasing visible light irradiation time. Moreover, the MB solution increasingly lost its color as the MB concentration continued to decrease. Two steps are involved in the photocatalytic decomposition of the dyes: adsorption of dye molecules and dye molecule degradation. After adsorption in the dark for 150 min with magnetic stirring, the samples were at adsorption-desorption equilibrium. In the degradation step, it can be clearly seen that 50% of MB was degraded by the Pt-graphene/TiO_2 nanocomposite. The MB degradation rate constant for Pt-graphene/TiO_2 was 6.54×10^{-3} min^{-1} under visible light irradiation, which value was much higher than those for TiO_2, TiO_2 and Pt/TiO_2.

In order to further demonstrate the photostability and cycle performance of the Pt-graphene/TiO_2 sample, circulating runs in the photocatalytic degradation of MB in the presence of Pt-graphene/TiO_2 under visible light were conducted. As shown in Fig. 6, the photocatalyst did not exhibit any significant loss of photocatalytic activity after 3 runs of MB degradation, which indicates that the Pt-graphene/TiO_2 photocatalyst had high stability and cannot be photocorroded during the photocatalytic oxidation of the MB solution. Thus, the Pt-graphene/TiO_2 composite photocatalyst is promising for practical applications in environmental purification. This graphene composite can improve not only the photocatalytic performance but also the long-term stability of the TiO_2 nanocrystals. This result is significant from the viewpoint of practical application because the enhanced photocatalytic activity and prevention of catalyst deactivation will lead to a more cost-effective operation.

4. Conclusions

In this study, we successfully synthesized Pt–graphene/TiO_2 nanocomposites with different weight ratios by a facile and fast ultrasonic assisted method. It is clear that the Pt–graphene/TiO_2 nanocomposite can be used as efficient photocatalyst under visible light irradiation. It is observed that the use of graphene and Pt in the composite increase the photocatalytic activity. The same phenomenon is observed in case of visible light irradiation. This high activity is also attributed to the synergetic effect of high charge mobility and the observed red shift in the absorption edge of the Pt–graphene/TiO_2 nanocomposites. It is hoped that our current work will offer a useful source of reference for the fabrication or design of graphene/TiO_2 nanocomposites decorated with noble metals, for application as photocatalysts in environment remediation.

References

1. K. V. Emtsev, A. Bostwick, K. Horn, J. Jobst, G. L. Kellogg, L. Ley, J. L. McChesney, T. Ohta, S. A. Reshanov, J. Röhrl, E. Rotenberg, A. K. Schmid, D. Waldmann, H. B. Weber, and T. Seyller, "Towards Wafer-Size Graphene Layers by Atmospheric Pressure Graphitization of Silicon Carbide," *Nat. Mater.*, **8** [3] 203-7 (2009).
2. H. Wang, G. Wang, P. Bao, S. Yang, W. Zhu, X. Xie, and W.-J. Zhang, "Controllable Synthesis of Submillimeter Single-Crystal Monolayer Graphene Domains on Copper Foils by Suppressing Nucleation," *J. Am. Chem. Soc.,* **134** [8] 3627-30 (2012).
3. J. P. hao, S. P. Pei, W. C. Ren, L. B. Gao, and H. M. Cheng, "Efficient Preparation of Large-Area Graphene Oxide Sheets for Transparent Conductive Films," *ACS Nano*, **4** [9] 5245-52 (2010).
4. A. Kasry, M. A. Kuroda, G. J. Martyna, G. S. Tulevski, and A. A. Bol, "Chemical Doping of Large-Area Stacked Graphene Films for Use as Transparent, Conducting Electrodes," *ACS Nano*, **4** [7] 3839-44 (2010).
5. L. G. Arco, Y. Zhang, C. W. Schlenker, K. M. Ryu, M. E.

Thompson, and C. W. Zhou, "Continuous, Highly Flexible, and Transparent Graphene Films by Chemical Vapor Deposition for Organicphotovoltaics," *ACS Nano*, **4** [5] 2865-73 (2010).
6. X. Wang, L. J. Zhi, N. Tsao, Z. Tomovic, J. L. Li, and K. Mullen, "Transparent Carbon Films as Electrodes in Organic Solar Cells," *Angew. Chem.,* **120** [16] 3032-34 (2008).
7. X. Y. Qi, K. Y. Pu, H. Li, X. Z. Zhou, S. X. Wu, Q. L. Fan, and B. Liu, "Amphiphilic Graphene Composites," *Angew. Chem., Int. Ed.*, **49** [49] 9426-29 (2010).
8. P. Sutter, "Epitaxial Graphene: How Silicon Leaves the Scene," *Nat. Mater*., **8** [3] 171-72 (2009) .
9. W. Poirier and F. Schopfer, "Can Graphene Set New Standards," *Nat. Nanotechnol.*, **5** [3] 171-72 (2010).
10. P. Maher, L. Wang, Y. Gao, C. Forsythe, T. Taniguchi, K. Watanabe, D. Abanin, Z. Papić, P. Cadden-Zimansky, J. Hone, P. Kim, and C. R. Dean, "Tunable Fractional Quantum Hall Phases in Bilayer Graphene," *Science*, **345** [6192] 61-4 (2014).
11. K. S. Kim, Y. Zhao, H. Jang, S. Y. Lee, J. M. Kim, K. S. Kim, J.-H. Ahn, P. Kim, J.-Y. Choi, and B. H. Hong, "Large-Scale Pattern Growth of Graphene Films for Stretchable Transparent Electrodes," *Nature,* **457** [7230] 706-10 (2009).
12. X. Li, W. Cai, J. An, S. Kim, J. Nah, D. Yang, R. Piner, A. Velamakanni, I. Jung, E. Tutuc, S. K. Banerjee, L. Colombo, and R. S. Ruoff "Large-Area Synthesis of High-Quality and Uniform Graphene Films on Copper Foils," *Science,* **324** [5932] 1310-14 (2009).
13. L. Gao, W. Ren, H. Xu, L. Jin, Z. Wang, T. Ma, L.-P. Ma, Z. Zhang, Q. Fu, L.-M. Peng, X. Bao, and H.-M. Cheng, "Repeated Growth and Bubbling Transfer of Graphene with Millimeter Size Single-Crystal Grains Using Platinum," *Nat. Commun.,* **3** 699 (2012).
14. P. W. Sutter, J. I. Flege, and E. A. Sutter, "Epitaxial Graphene on Ruthenium," *Nat. Mater.,* **7** [5] 406-11 (2008).
15. Q. Yu, J. Lian, S. Siriponglert, H. Li, Y. P. Chen, and S.-S. Pei, "Graphene Segregated on Ni Surfaces and Transferred to Insulators," *Appl. Phys. Lett.*, **93** [11] 113103 (2008).
16. K. S. Kim, Y. Zhao, H. Jang, S. Y. Lee, J. M. Kim, K. S. Kim, J.-H. Ahn, P. Kim, J.-Y. Choi, and B. H. Hong, "Large-Scale Pattern Growth of Graphene Films for Stretchable Transparent Electrodes," *Nature*, **457** [7230] 706-10 (2009).
17. A. Reina, X. Jia, J. Ho, D. Nezich, H. Son, V. Bulovic, M. S. Dresselhaus, and J. Kong, "Large Area, Few-Layer Graphene Films on Arbitrary Substrates by Chemical Vapor Deposition," *Nano Lett.,* **9** [1] 30-5 (2009).
18. H. L. Wang, L. F. Cui, Y. Yang, H. S. Casalongue, J. T. Robinson, Y. Liang, Y. Cui, and H. Dai, "Mn_3O_4-Graphene Hybrid as a High-Capacity Anode Materials for Lithium Ion Batteries," *J. Am. Chem. Soc.,* **132** [40] 13978-80 (2010).
19. P. K. Ang, W. Chen, A. T. S. Wee, and K. P. Loh, "Solution-Gated Epitaxial Graphene as pH Sensor," *J. Am. Chem. Soc.,* **130** [44] 14392-93 (2008).
20. S. F. Hou, M. L. Kasner, S. J. Su, K. Patel, and R. Cuellari, "Highly Sensitive and Selective Dopamine Biosensor Fabricated with Silanized Graphene," *J. Phys. Chem. C,* **114** [35] 14915-21 (2010).
21. S. Liu, M.-Q. Yang, and Y.-J. Xu, "Surface Charge Promotes the Synthesis of Large, Flat Structured Graphene–(CdS Nanowire)–TiO_2 Nanocomposites as Versatile Visible Light Photocatalysts," *J. Mater. Chem. A,* **2** 430-40 (2014).
22. J. Aguado, R. Van Grieken, M. J. Lopez-Munos, and J. Marugan, "A Comprehensive Study of the Synthesis, Characterization and Activity of TiO_2 and Mixed TiO_2/SiO_2 Photocatalysts," *Appl. Catal., A*, **312** 202-12 (2006).
23. J. Coraux, A. T. N. Diaye, C. Busse, and T. Michely, "Structural Coherency of Graphene on Ir (111)," *Nano Lett.,* 8 [2] 565-70 (2008).
24. C. Berger, Z. Song, X. Li, X. Wu, N. Brown, C. Naud, D. Mayou, T. Li, J. Hass, A. N. Marchenkov, E. H. Conrad, P. N. First, and W. A. de Heer, "Electronic Confinement and Coherence in Patterned Epitaxial Graphene," *Science,* **312** [5777] 1191-96 (2006)
25. K. A. Ritter and J. W. Lyding, "The Influence of Edge Structure on the Electronic Properties of Graphene Quantum Dots and Nanoribbons," *Nat. Mater.*, **8** [3] 235-42 (2009).
26. C. Tao, L. Jiao, O. V. Yazyev, Y.-C. Chen, J. Feng, X. Zhang, R. B. Capaz, J. M. Tour, A. Zettl, S. G. Louie, H. Dai, and M. F. Crommie, "Spatially Resolving Edge States of Chiral Graphene Nanoribbons," *Nat. Phys.*, **7** 616-20 (2011).
27. M. Pan, E. C. Girão, X. Jia, S. Bhaviripudi, Q. Li, J. Kong, V. Meunier, and M. S. Dresselhaus, "Topographic and Spectroscopic Characterization of Electronic Edge States in CVD Grown Graphene Nanoribbons," *Nano Lett.*, **12** [4] 1928-33 (2012).
28. X. Zhang, O. V. Yazyev, J. Feng, L. G. Xie, C. G. Tao, Y.-C. Chen, L. Jiao, Z. Pedramrazi, A. Zettl, S. G. Louie, H. Dai, and M. F. Crommie, "Experimentally Engineering the Edge Termination of Graphene Nanoribbons," *ACS Nano,* **7** [1] 198-202 (2013).
29. A. C. Ferrari and D. M. Basko, "Raman Spectroscopy as a Versatile Tool for Studying the Properties of Graphene," *Nat. Nanotechnol.*, **8** [4] 235-46 (2013).
30. A. C. Ferrari, J. C. Meyer, V. Scardaci, C. Casiraghi, M. Lazzeri, F. Mauri, S. Piscanec, D. Jiang, K. S. Novoselov, S. Roth, and A. K. Geim, "Raman Spectrum of Graphene and Graphene Layers," *Phys. Rev. Lett.,* **97** [18] 187401 (2006).
31. K. Ullah, S. Ye, S.-G. Kim, B.-J. Lee, E.-H.Yoon, Y.-R. Kim, B.-S. Kim, and W-C. Oh, "Additional Materials Effect for Improved Electrochemical Performance of Active Carbon Fiber based Electric Double Layer Capacitors," *Asian J. Chem.,* **27** [6] 2260-66 (2015).
32. K. Uallah, A. Ali, S. Ye, L. Zhu, I.-J. Kim, S.-H. Yang, and W.-C. Oh, "Electrochemical Performance of Graphene/Active Carbon based Electric Double Supercapacitor," *Asian J. Chem.,* **28** [1] 133-37 (2016).
33. L. Gong, I. A. Kinloch, R. J. Young, I. Riaz, R. Jalil, and K. S. Novoselov, "Interfacial Stress Transfer in a Graphene Monolayer Nanocomposite," *Adv. Mater.*, **22** [24] 2694-97 (2010).
34. V. Panchal, L. Manzin, Y. Tzalenchuk, and O. Kazakova, "Visualisation of Edge Effects in Side-Gated Graphene Nanodevices," *Sci. Rep.,* **4** 5881 (2014).